Supporting information for

Defect Formation and Microstructure Tuning via Proton Irradiation to Control Electrochemical and Phase Reversibility in Layered Battery Materials

Muhammad Mominur Rahman,[1,2*] Hyosim Kim,[3] Matthew Chancey,[3] Vivek Thampy,[4] Anyang Hu,[1] Luxi Li,[5] Lu Ma,[6] Enyuan Hu,[7] Sami Sainio,[4] Dennis Nordlund,[4] Sooyeon Hwang,[8] Yongqiang Wang,[3] Xian-Ming Bai,[9] and Feng Lin[1,9,10*]

1. Department of Chemistry, Virginia Tech, Blacksburg, VA 24061, USA
2. Electrification Section, Electrification and Energy Infrastructure Division, Oak Ridge National Laboratory, TN 37932, USA
3. Materials Science and Technology Division, Los Alamos National Laboratory, Los Alamos, NM 87545, USA
4. Stanford Synchrotron Radiation Lightsource, SLAC National Accelerator Laboratory Menlo Park, CA 94025, USA
5. Advanced Photon Source, Argonne National Laboratory, Lemont, IL 60439, USA
6. National Synchrotron Light Source II, Brookhaven National Laboratory, Upton, NY 11973, USA
7. Chemistry Division, Brookhaven National Laboratory, Upton, NY 11973, USA
8. Center for Functional Nanomaterials, Brookhaven National Laboratory, Upton, NY 11973, USA
9. Department of Materials Science and Engineering, Virginia Tech, Blacksburg, VA 24061, USA
10. School of Engineering, Brown University, Providence, Rhode Island 02912, USA

Email: rahmanm1@ornl.gov, feng_lin@brown.edu

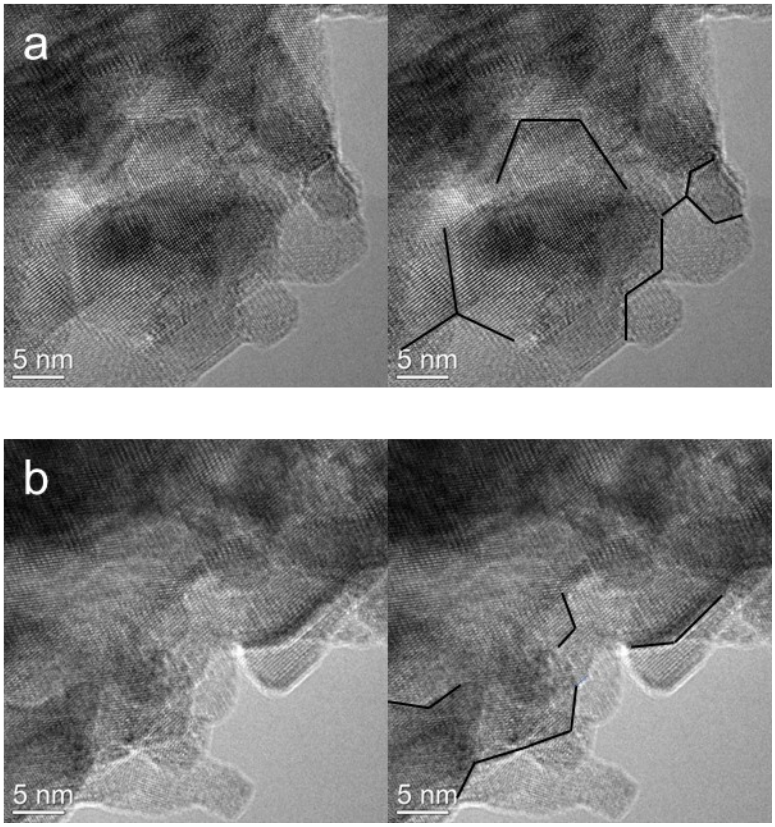

Figure S1. (a-b) Transmission electron microscopy (TEM) images of 0.01 dpa proton irradiated $Na_{2/3}Fe_{1/2}Mn_{1/2}O_2$ (left) and images with some guidelines to show a few of the crystalline nanodomains (right).

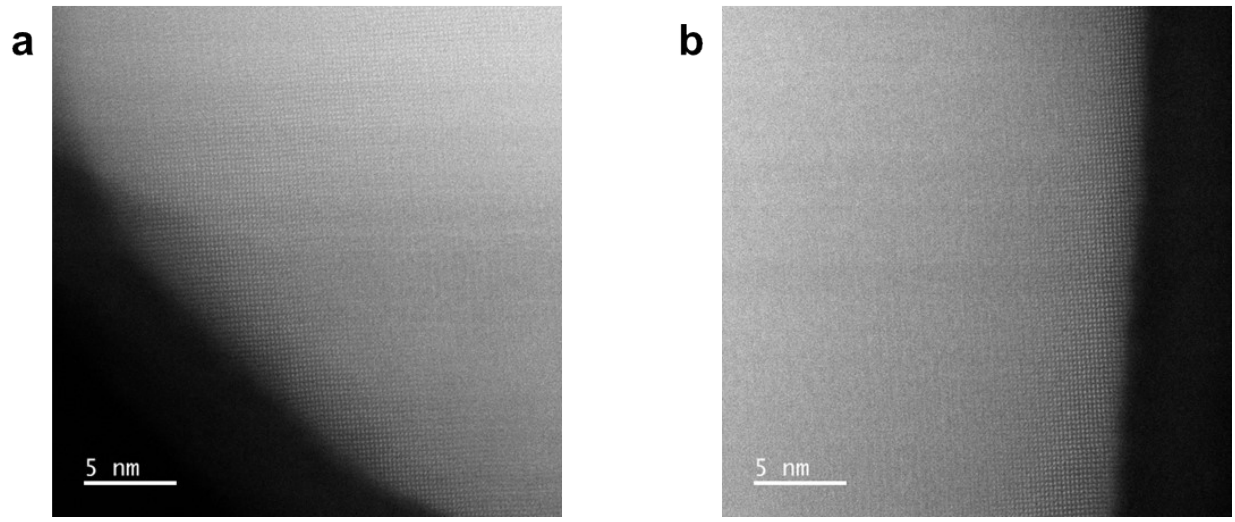

Figure S2. (a-b) TEM images of pristine unirradiated $Na_{2/3}Fe_{1/2}Mn_{1/2}O_2$.

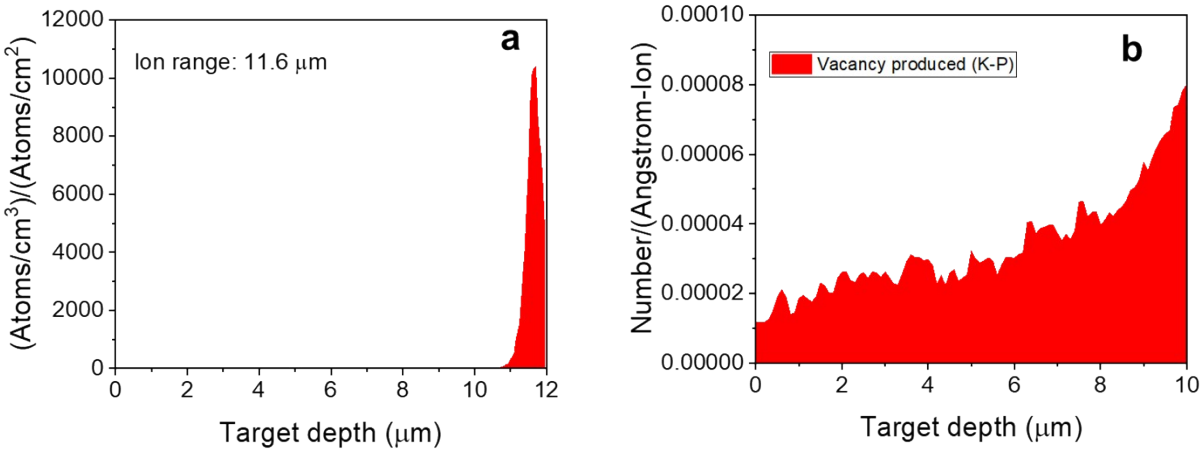

Figure S3. Stopping and Range of Ions in Matter (SRIM) calculation for (a) ion distribution and (b) damage events of 1.1 MeV proton in $Na_{2/3}Fe_{1/2}Mn_{1/2}O_2$. 100,000 protons were used to perform the calculation. Ion distribution shows a range of 11.6 μm, larger than the electrode thickness excluding the current collector (10 μm). Therefore, minimum implanted protons within the active material can be expected. Since the electrode thickness was 10 μm, vacancy distribution is shown for up to this distance.

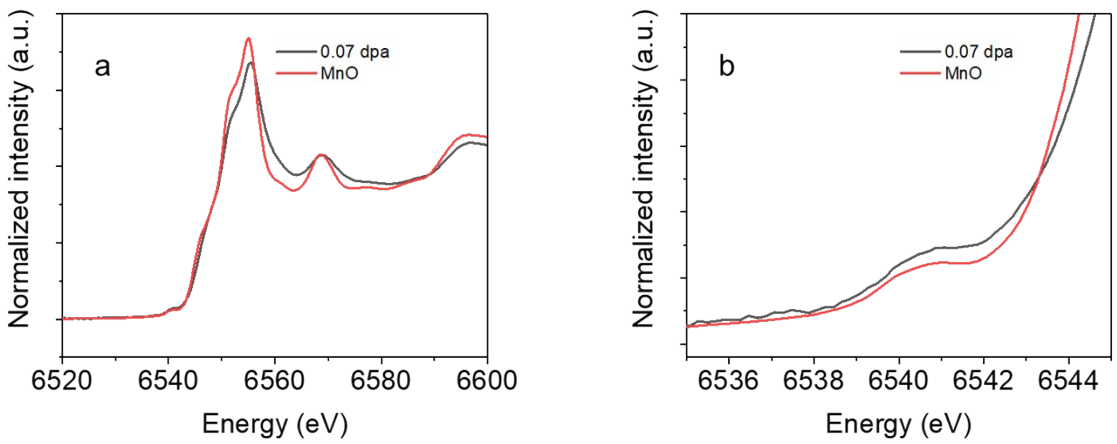

Figure S4. (a) Mn K-edge X-ray absorption near edge structure (XANES) spectra of MnO and 0.07 dpa proton irradiated $Na_{2/3}Fe_{1/2}Mn_{1/2}O_2$. (b) Pre-edge region of Mn K-edge XANES spectra of MnO and 0.07 dpa proton irradiated $Na_{2/3}Fe_{1/2}Mn_{1/2}O_2$.

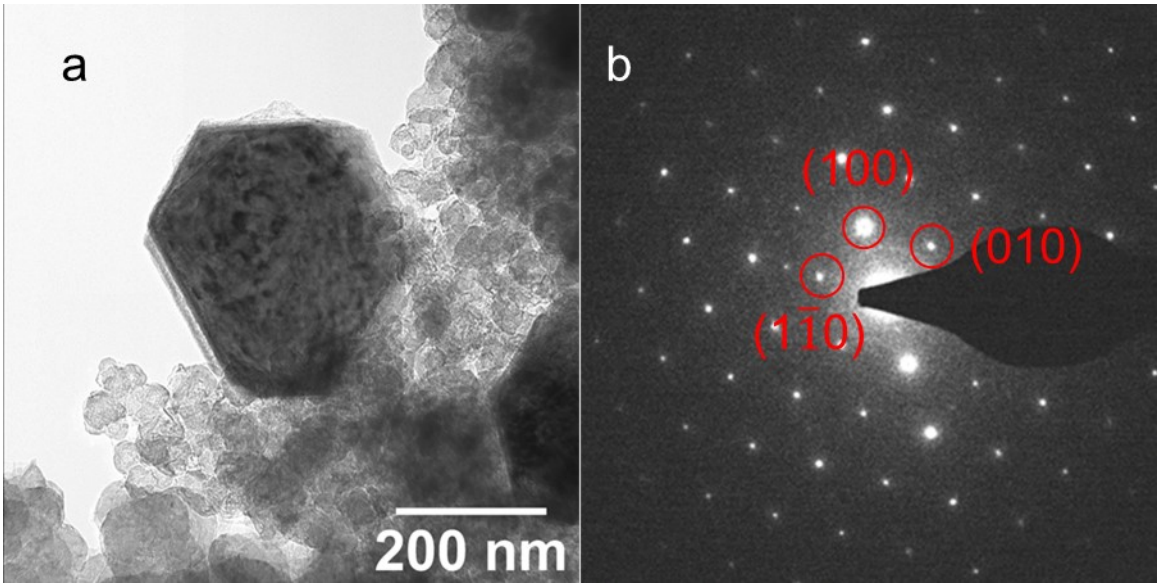

Figure S5. (a) Unirradiated particle of $Na_{2/3}Fe_{1/2}Mn_{1/2}O_2$. The small more transparent particles surrounding the particle are carbon black. (b) Electron diffraction pattern of the particle in (a) along the <001> zone axis.

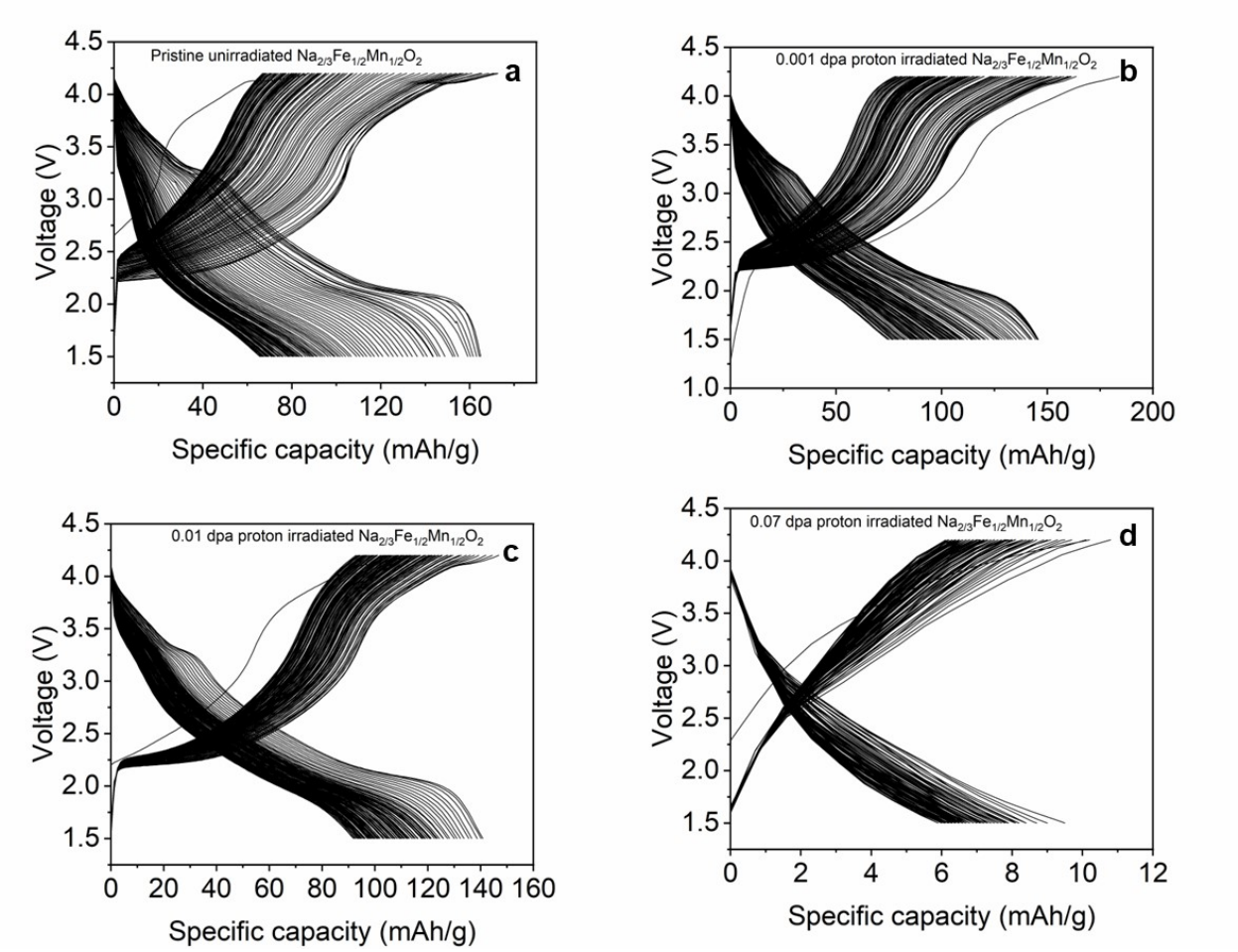

Figure S6. Charge-discharge curves up to 100 cycles of (a) unirradiated, (b) 0.001 dpa proton irradiated, (c) 0.01 dpa proton irradiated, and (d) 0.07 dpa proton irradiated $Na_{2/3}Fe_{1/2}Mn_{1/2}O_2$ in Na cell at C/2 rate.

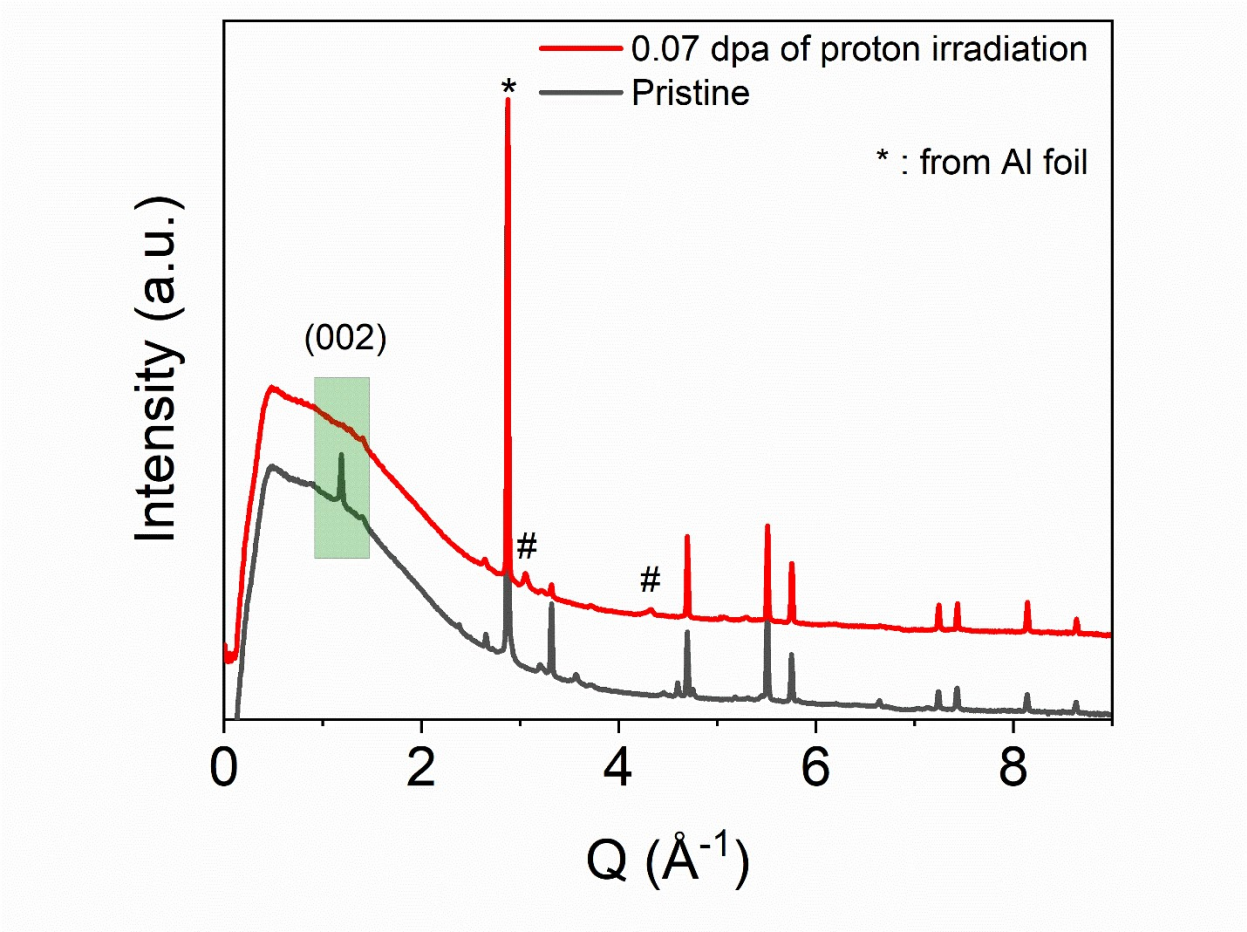

Figure S7. Ex situ XRD patterns of the unirradiated (pristine) and 0.07 dpa proton irradiated $Na_{2/3}Fe_{1/2}Mn_{1/2}O_2$. The (002) peak is absent in the 0.07 dpa material, indicating deterioration of the layered structure. Also, new peaks in the pattern (marked by "#") indicates new phase formation.

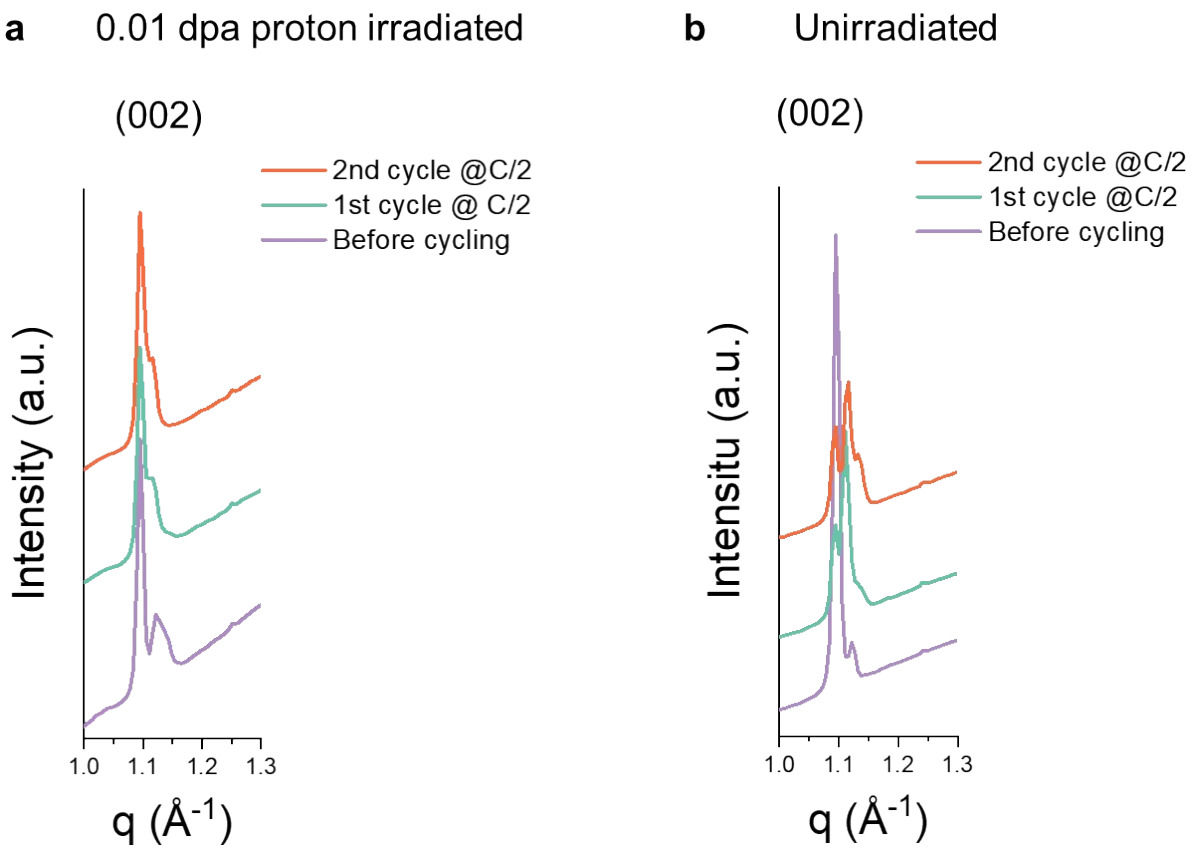

Figure S8. Evolution of the (002) Bragg peak of (a) 0.01 dpa proton irradiated, and (b) unirradiated ($Na_{2/3}Fe_{1/2}Mn_{1/2}O_2$) before and after cycling in Na cells. Intensity reported here is the absolute intensity of the peaks.

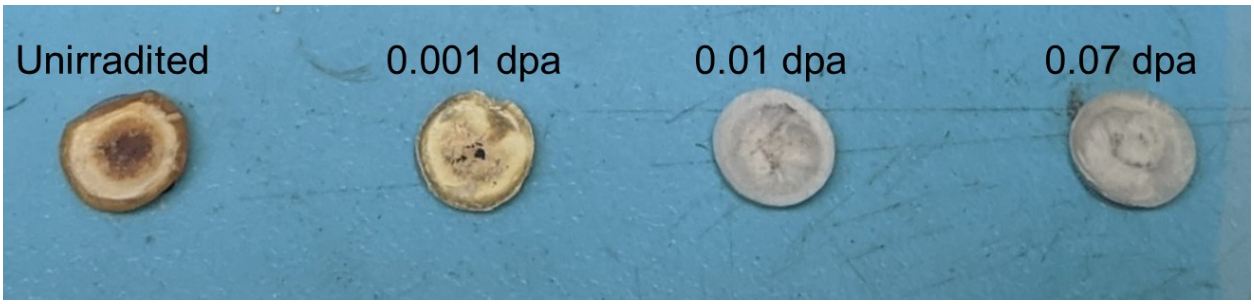

Figure S9. Digital photograph of glass fiber separator after electrochemical cycling in batteries with unirradiated and proton irradiated $Na_{2/3}Fe_{1/2}Mn_{1/2}O_2$ cathodes for 500 cycles at C/2 rate. The color change of the glass fiber separator from the first two samples comes from transition metal dissolution. The 0.07 dpa sample did not provide meaningful capacity and thus the dissolution is also limited.